



ELSEVIER

Available online at www.sciencedirect.com

Journal of Magnetism and Magnetic Materials 320 (2008) 695–698

www.elsevier.com/locate/jmmm

Spatial determination of magnetic avalanche ignition points

Reem Jaafar^a, S. McHugh^a, Yoko Suzuki^a, M.P. Sarachik^{a,*}, Y. Myasoedov^b, E. Zeldov^b,
H. Shtrikman^b, R. Bagai^c, G. Christou^c

^aPhysics Department, City College of the City University of New York, New York, NY 10031, USA

^bDepartment Condensed Matter Physics, The Weizmann Institute of Science, Rehovot 76100, Israel

^cDepartment of Chemistry, University of Florida, Gainesville, FL 32611, USA

Received 9 July 2007

Available online 30 August 2007

Abstract

Using time-resolved measurements of local magnetization in the molecular magnet $\text{Mn}_{12}\text{-ac}$, we report studies of magnetic avalanches (fast magnetization reversals) with non-planar propagating fronts, where the curved nature of the magnetic fronts is reflected in the time-of-arrival at micro-Hall sensors placed at the surface of the sample. Assuming that the avalanche interface is a spherical bubble that grows with a radius proportional to time, we are able to locate the approximate ignition point of each avalanche in a two-dimensional cross-section of the crystal. We find that although in most samples the avalanches ignite at the long ends, as found in earlier studies, there are crystals in which ignition points are distributed throughout an entire weak region near the center, with a few avalanches still originating at the ends.

© 2007 Elsevier B.V. All rights reserved.

PACS: 71.30.+h; 73.40.Qv; 73.50.Jt

Keywords: Magnetism; Molecular magnet; Magnetic avalanche; Magnetic deflagration; Magnetic relaxation

$\text{Mn}_{12}\text{-acetate}$, or $[\text{Mn}_{12}\text{O}_{12}(\text{CH}_3\text{COO})_{16}(\text{H}_2\text{O})_4] \cdot 2\text{CH}_3\text{COOH} \cdot 4\text{H}_2\text{O}$ (hereafter, referred to as $\text{Mn}_{12}\text{-ac}$), is a prototypical molecular magnet composed of magnetic molecules with cores consisting of 12 Mn atoms strongly coupled by exchange to form superparamagnetic clusters of large spin $S = 10$ at low temperatures [1,2]. Arranged in a centered tetragonal lattice, the Mn_{12} clusters are subject to strong magnetic anisotropy along the symmetry axis (the c -axis of the crystal). Below the blocking temperature of about 3.5 K, the crystal exhibits remarkable staircase magnetic hysteresis due to resonant quantum spin tunneling between energy levels on opposite sides of the anisotropy barrier corresponding to different spin projections along the easy axis [3].

Recent local time-resolved measurements of fast magnetization reversal in single crystals of $\text{Mn}_{12}\text{-ac}$ have shown that a magnetization avalanche spreads as a narrow interface that propagates through the crystal at a constant

velocity that is roughly two orders of magnitude smaller than the speed of sound [4]. This has been attributed to “magnetic deflagration”, in analogy with the propagation of a flame front through a flammable chemical substance, a phenomenon called chemical deflagration [5]. The avalanches in these studies [4] occurred stochastically in response to a time-varying (swept) magnetic field applied along the easy axis of the $\text{Mn}_{12}\text{-ac}$ crystals. For the experimental conditions and samples used, the avalanches originated at or near the long end of the crystal. In a recent study using surface acoustic waves to ignite avalanches at fixed magnetic fields, Hernandez-Minguez et al. [6] deduced the velocity of avalanches as a function of applied magnetic field by assuming, based on the finding of Suzuki et al. [4], that the avalanches were triggered at the long end and traveled the full length of their $\text{Mn}_{12}\text{-ac}$ crystals. Using this assumption, the velocity was shown to display maxima which were attributed to “deflagration assisted by quantum tunneling” at the resonant fields corresponding to the steps observed in the magnetic hysteresis [3].

*Corresponding author. Tel.: +1 212 650 5618; fax: +1 212 650 6940.

E-mail address: sarachik@sci.cny.cuny.edu (M.P. Sarachik).

The cause of the avalanches—where they originate, how they nucleate, and how they ignite—is one of the most interesting questions in this field. In the experiments of Suzuki et al. [4], equally spaced micron-sized Hall bars placed near the middle of the long dimension (*c*-axis) of a $\text{Mn}_{12}\text{-ac}$ crystal registered signals at approximately equal time intervals, indicating the propagation of a planar (or approximately planar) magnetic front. This implied that the avalanches were triggered well outside the central region of the sample, and they were assumed to originate at or near the end. The local position of the trigger points could not be determined. In this paper we report a study of avalanches triggered in a swept magnetic field for which the time-of-arrival of the signal at the Hall bars is not equally spaced, implying the propagation of magnetic spin-reversal along a curved front. Assuming that the velocity of propagation of an avalanche is isotropic and gives rise to a spherical propagating front, the time-of-arrival at sensors placed at the surface of the sample allowed us to trace each avalanche back to its approximate point of ignition. We find that although in most samples the avalanches ignite at the long ends, there are crystals in which ignition points are distributed throughout an entire weak region near the center, with a few avalanches still originating at the ends.

The experimental system is described in detail in Ref. [4]. Small Hall bars (six or seven, depending on the sample) of dimensions $30 \times 30 \mu\text{m}^2$ placed at $80 \mu\text{m}$ (center to center) intervals were used to measure the magnetization of single crystals of $\text{Mn}_{12}\text{-ac}$ in the form of parallelepipeds of typical cross section $0.3 \times 0.3 \text{ mm}^2$ and length 1–1.4 mm. Operating at 0.255 K, avalanches were recorded for magnetic fields between 1.5 and 3.5 T. The Hall sensors were aligned to detect the magnetic induction of the sample in the *x*-direction, B_x , which is proportional to the spatial derivative of M_z in the region near the sensor, $B_x \propto \partial M_z / \partial z$ [7]. B_x is proportional M_z , and for a uniform magnetization in the *z*-direction, derives mostly from the strong gradient at the sample ends. During an avalanche, there is a large contribution to B_x at the front, the narrow propagating interface between regions of opposing magnetization, where $\partial M_z / \partial z$ is large. Each sensor thus registers a large signal as the front passes by. The sign of the peak, positive or negative, is determined by the direction of the field lines.

Fig. 1 shows the time evolution of an avalanche starting from some region away from the Hall sensors near the end of the sample. The schematic (top center) shows the magnetization of the crystal and the field lines that give rise to the observed signal. The graphed inset shows the peak

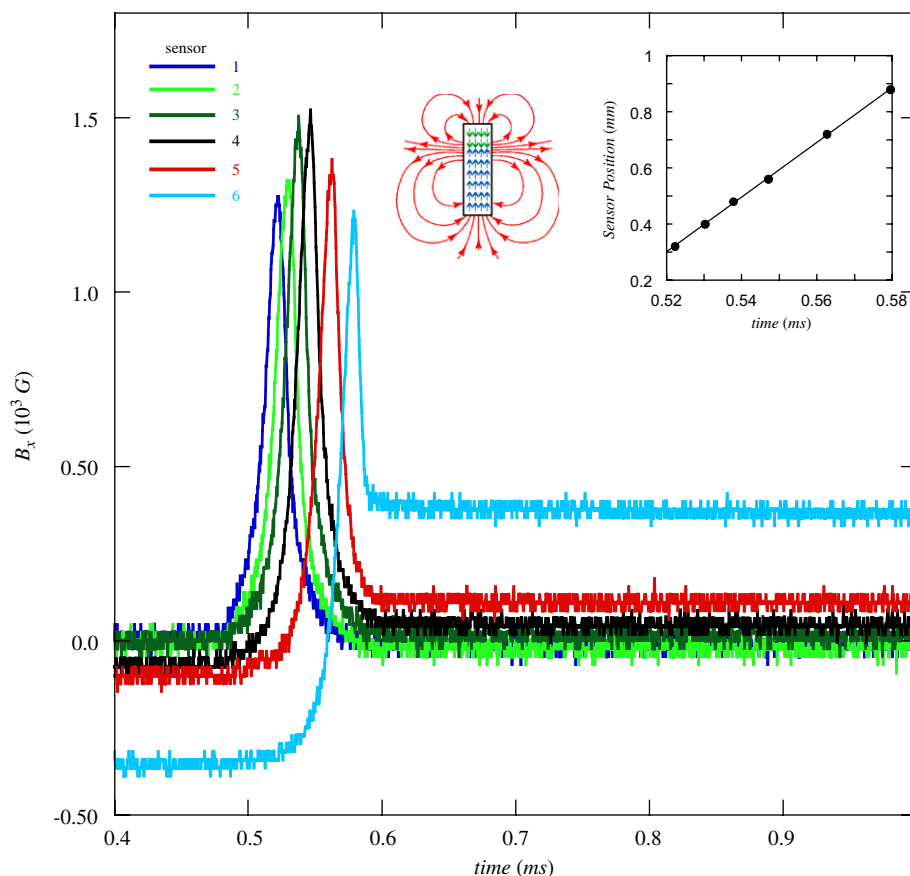


Fig. 1. Signals recorded during a magnetic avalanche by Hall sensors placed on the surface near the middle of a bar-shaped sample of $\text{Mn}_{12}\text{-acetate}$. The schematic indicates the field line configuration that gives rise to the signals as the avalanche propagates from one end of the sample to the other. The inset shows sensor positions versus the time at which each sensor recorded the peak amplitude for an avalanche that started at the top and travels downward.

position of the signal plotted as a function of time; the slope of the straight line yields the velocity of propagation of the front. These data are consistent with the results of Ref. [4].

Fig. 2 shows the sensor traces for an avalanche observed in a different sample that produces both positive and negative signals. As before, we plot the positions of the peaks as a function of time for two such avalanches in Fig. 3. In contrast with the straight line shown in the inset to Fig. 1, which we have attributed to the planar front of an avalanche propagating from the end of the sample, we see a “V-shaped” curve with negative and positive curved branches. This can be understood as an avalanche starting near the middle of the sample and propagating in opposite directions toward the sample ends. As illustrated in the schematic inset in Fig. 2, the signals of opposite sign are due to field lines pointing in opposite directions corresponding to the upper (lower) front traveling upward (downward). Fig. 3(a) shows an avalanche initiating above the third Hall sensor while Fig. 3(b) shows one originating between the fourth and fifth. The avalanches of Fig. 3 clearly show curvature absent from the planar front of Fig. 1 and are distinctly different from one another. We propose that the curvature is determined by the distance from the ignition point to the surface on which the Hall

sensors are mounted. This can be understood by simple geometric considerations.

We assume the avalanche grows as a spherical bubble with a radius growing linearly in time, $r = vt$. In other words,

$$v^2 t^2 = (x - x_0)^2 + (y - y_0)^2 + (z - z_0)^2,$$

where (x_0, y_0, z_0) is the ignition point within the sample. With Hall bars along the z -axis and $y = x = 0$, the position of the peak as a function of time is given as the intersection of the spherical bubble with the z -axis,

$$z(t) = z_0 \pm \sqrt{v^2 t^2 - d^2}, \tag{1}$$

where d is the distance $\sqrt{(y_0)^2 + (x_0)^2}$ between the point of ignition and the z -axis containing the Hall sensor array.

By fitting the peak positions in time with this expression, we can extract values of z_0 and d , and thereby determine the point where the avalanche started. Thus, for example, frames (a) and (b) of Fig. 3 show data with distinctly different curvatures for two different avalanches originating within the same sample. As illustrated in the schematic diagrams, the smaller curvature of Fig. 3(a) is caused by an avalanche triggered near the surface on which the sensors are mounted, while the larger curvature of Fig. 3(b) is due to an avalanche originating further away.

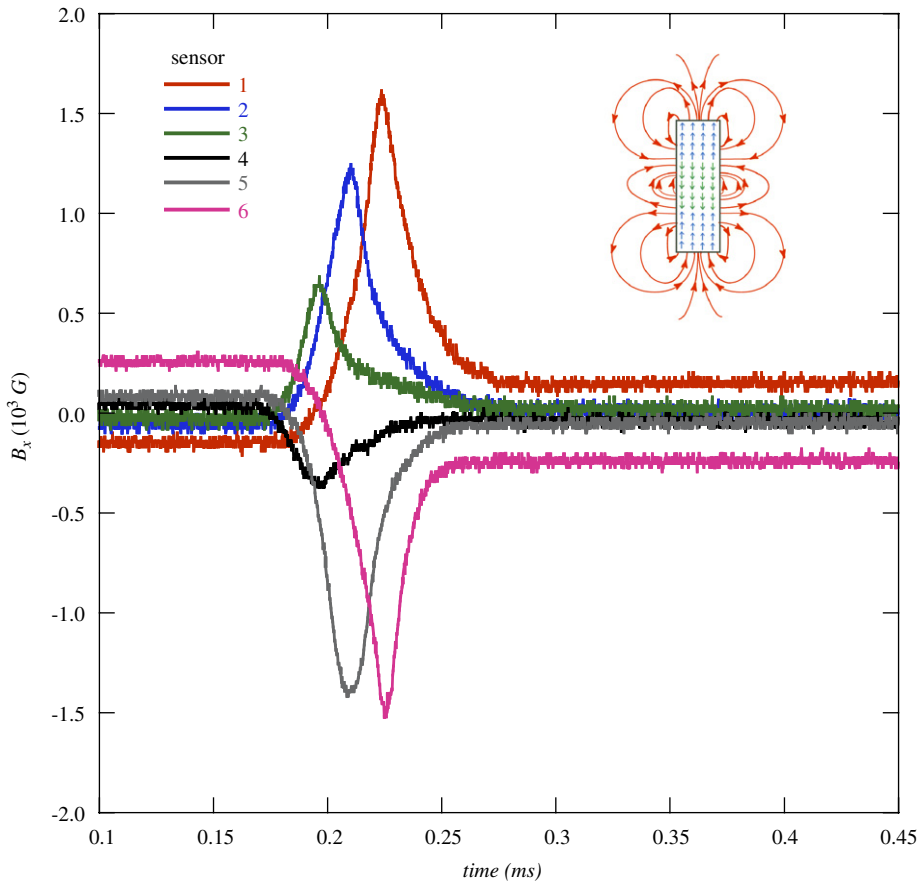


Fig. 2. Sensor signals for an avalanche starting near the middle of the sample. The schematic indicates the (quadrupolar) field configuration associated with avalanche fronts propagating in opposite directions toward the two ends, giving rise to the observed positive-going and negative-going signals.

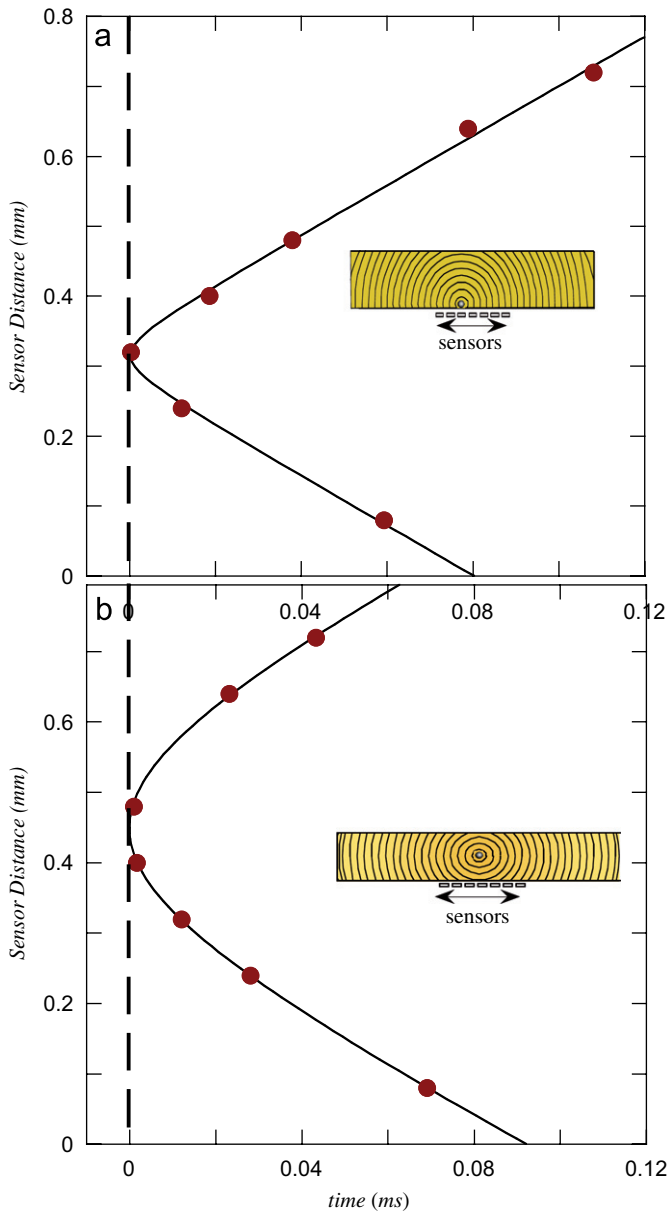


Fig. 3. For two avalanches, the sensor position is shown as a function of the time of arrival of the peak amplitude at each sensor, where $t = 0$ is arbitrarily chosen to be the time of arrival of the front at the z -axis. In contrast with the inset shown in Fig. 1, the traces are not straight lines, and the curvature is different for the avalanches shown in frame (a) (b). As shown in the text, frame (a) corresponds to an avalanche triggered near the surface while frame (b) shows an avalanche triggered far from the surface on which the sensor was mounted.

For a particular sample of dimensions $1.4 \times 0.3 \times 0.3 \text{ mm}^3$, Fig. 4 shows a distribution of the avalanche ignition points projected onto the d - z plane. Hall sensors were placed near the middle of the sample extending from $z \approx 0.4$ to 1.0 mm . The vertical lines near the ends of the sample indicate “blind” regions outside the Hall sensor array where avalanches could not be traced back to their origin. Only $\approx 5\%$ of the avalanches were triggered in these regions. For this sample, the ignition points lie

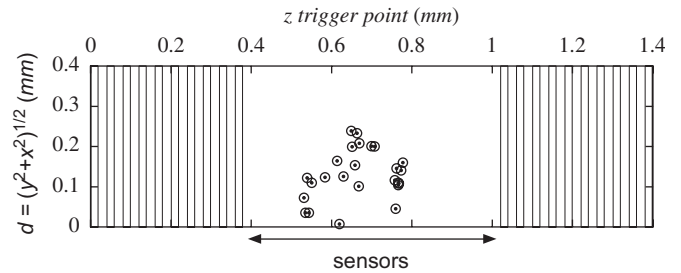


Fig. 4. Distribution of ignition points of avalanches for a particular sample projected onto the d - z plane. The double arrow indicates the region spanned by Hall sensors; the vertical lines designate the regions beyond the Hall sensor array where avalanches could not be traced to their points of origin.

predominantly within a region near the center of radius roughly $150 \mu\text{m}$.

To summarize, we report a study that provides information about the location and distribution of ignition points of propagating avalanches corresponding to rapid spin reversal in the molecular magnet $\text{Mn}_{12}\text{-ac}$ [8]. In most of the crystals studied, the avalanches originated predominantly from somewhere near the ends. On the other hand, in some crystals the avalanches ignited near the center of the long axis (with a few still coming from the ends). Contrary to the simple expectation that the ignition points are determined by one or several weak spots associated with local defects, or locally tilted axes, or a high local density of the “second species” ubiquitous in $\text{Mn}_{12}\text{-ac}$, we find that the ignition points are instead distributed randomly throughout a substantial part of these sample.

This work was supported at City College by NSF Grant DMR-00451605. E.Z. and H.S. acknowledge the support of the Israel Ministry of Science, Culture and Sports. Support for G.C. was provided by NSF Grant CHE-0414555.

References

- [1] T. Lis, Acta. Cryst. B 69 (1980) 2042.
- [2] R. Sessoli, D. Gatteschi, A. Caneschi, M.A. Novak, Nature (London) 365 (1993) 141.
- [3] J.R. Friedman, M.P. Sarachik, J. Tejada, R. Ziolo, Phys. Rev. Lett. 76 (1996) 3830.
- [4] Y. Suzuki, M.P. Sarachik, E.M. Chudnovsky, S. McHugh, R. Gonzalez-Rubio, N. Avraham, Y. Myasoedov, E. Zeldov, H. Shtrikman, N.E. Chakov, G. Christou, Phys. Rev. Lett. 95 (2005) 147201.
- [5] L.D. Landau, E.M. Lifshitz, Fluid Dynamics, Pergamon, New York, 1987.
- [6] A. Hernandez-Minguez, J.M. Hernandez, F. Macia, A. Garcia-Santiago, J. Tejada, P.V. Santos, Phys. Rev. Lett. 95 (2005) 217205.
- [7] N. Avraham, A. Stern, Y. Suzuki, K.M. Mertes, M.P. Sarachik, E. Zeldov, Y. Myasoedov, H. Shtrikman, E.M. Rumberger, D.N. Hendrickson, N.E. Chakov, G. Christou, Phys. Rev. B 72 (2005) 144428.
- [8] A. Hernandez-Minguez, F. Macia, J.M. Hernandez, J. Tejada, L.H. He, F.F. Wang, Europhys. Lett. 75 (2006) 811.